Int. J. Appl. Math. Comput. Sci., 2011, Vol. 21, No. 4, 703–715
DOI: 10.2478/v10006-011-0056-4

ESTIMATION OF FEEDWATER HEATER PARAMETERS BASED ON A GREY–BOX APPROACH

TOMASZ BARSZCZ, PIOTR CZOP

Department of Robotics and Mechatronics
AGH University of Science and Technology, Al. Mickiewicza 30, 30–059 Cracow, Poland
e-mail: piotr.czop@labmod.com

The first-principle modeling of a feedwater heater operating in a coal-fired power unit is presented, along with a theoretical discussion concerning its structural simplifications, parameter estimation, and dynamical validation. The model is a part of the component library of modeling environments, called the Virtual Power Plant (VPP). The main purpose of the VPP is simulation of power generation installations intended for early warning diagnostic applications. The model was developed in the Matlab/Simulink package. There are two common problems associated with the modeling of dynamic systems. If an analytical model is chosen, it is very costly to determine all model parameters and that often prevents this approach from being used. If a data model is chosen, one does not have a clear interpretation of the model parameters. The paper uses the so-called grey-box approach, which combines first-principle and data-driven models. The model is represented by nonlinear state-space equations with geometrical and physical parameters deduced from the available documentation of a feedwater heater, as well as adjustable phenomenological parameters (i.e., heat transfer coefficients) that are estimated from measurement data. The paper presents the background of the method, its implementation in the Matlab/Simulink environment, the results of parameter estimation, and a discussion concerning the accuracy of the method.

Keywords: first-principle model, system identification, heater, heat exchanger, grey-box.

1. Introduction

In 2005, a large national research project DIADYN was initiated by a consortium of Polish technical universities and research institutes, involving 40 research teams. The main objective of the DIADYN project is to build an "integrated dynamic system of risk assessment, diagnostics and control of structures and technological processes". Within the framework of the project, the Virtual Power Plant (VPP) modeling environment has been developed (Barszcz, 2007) and has become an innovative approach for reconstructing the operational characteristics of a power plant unit, based on model and recorded process data. The VPP, described by Barszcz and Czop (2007), provides an environment for integrating a range of models of power plant components, data management systems and visualization methods into a standalone system.

The VPP became a part of the DIADYN project as a practical laboratory facilitating validation of a diagnostic methodology implemented as software algorithms or available in the form of hardware, for instance, as controllers with embedded fault detection and isolation algorithms. The novelty of the proposed simulation environment lies in the scope in which model-based diagnostics (Bonivento, 2001), recently one of the fastest developing technologies in the power generation sector, is supported.

The available results of numerous analytical and experimental studies are not sufficient to establish the feasibility of using a model-based approach to predict behavior and to diagnose large industrial installations, like power plants (Bonivento *et al.*, 2001; Bradatsch *et al.*, 1993; Korbicz *et al.*, 2004). Key problems encountered in practical implementation of such models are twofold. The first group of problems regards developing a model where, in most cases, even if the underlying physical equations are known, the correct values of parameters, and thus correct model behavior, are difficult to identify. On the other hand, for the "black-box" system identification approach, a sufficient amount of data covering the entire operation range is necessary but very difficult to collect. The second group of problems is related to the lack of a flexible work environment. The process of model development and consecutive diagnostic activities require efficient cooperation of specialists from different fields: power plant staff to

deliver data and technical documentation and diagnostics experts to model the process and draw conclusions. Results generated by the model should be presented to power plant experts and management in a comprehensible way; in practice, however, a set of heterogeneous software tools is used to perform these tasks, making the whole process hard to manage and inefficient.

The VPP is an environment tailored to properly emulate the functionality of a power plant unit. It is characterized by (i) a flexible structure enabling multiple configurations to be defined, (ii) an ability to import data acquired at the object, (iii) the possibility to store models of each component in different versions, (iv) for models of moderate complexity, an ability to achieve performance close to the real time, and (v) an ability to present results in either an advanced or a simplified form, for experts and operational staff of power plants, respectively.

The paper is divided into seven sections. Section 2 contains a classification of grey-box modeling methods and a survey of possible applications. Section 3 describes a model of a feedwater heater and Section 4 provides detailed methodology suitable for system identification of this model. Section 5 deals with aspects of system identification of a heater model presenting the results of model adjustment based on operational data from a power plant and the case-based sensitivity analysis of the model. Section 6 discusses the obtained results of system identification. Lastly, Section 7 presents the summary of the paper.

Nomenclature

$\dot{m}$ mass flux $[\mathrm{kg{\cdot}s^{-1}}]$

$\dot{Q}$ energy flux $[\mathrm{J{\cdot}s^{-1}}]$

ρ density $[\mathrm{kg{\cdot}m^{3}}]$

θ unknown parameter vector used in a general representation of a first-principle model

A heat exchange area $[\mathrm{m^2}]$

H internal energy $[\mathrm{J}]$

h enthalpy $[\mathrm{J{\cdot}kg^{-1}}]$

k heat exchange coefficient $[\mathrm{W{\cdot}m^{-2}{\cdot}K^{-1}}]$

p pressure $[\mathrm{Pa}]$

T temperature $[\mathrm{K}]$

$u(t)$ control vector used in a general representation of a first-principle model

V chamber volume $[\mathrm{m^3}]$

$w(t), v(t)$ sequences of independent random variables

$x(t)$ state vector used in a general representation of a first-principle model

$y(t)$ output vector used in a general representation of a first-principle model

Abbreviations

PID Proportional-Integral-Derivative controller

SSE Sum Squared Error

VPP Virtual Power Plant

2. Classification of grey-box modeling methods and a survey of applications

A classification and taxonomy of grey-box models was proposed by Sohlberg and Jacobsen (2008) and relies on an observation that, for many industrial processes, there is first-principle or heuristic, but incomplete, knowledge about the system. The work presented by Sohlberg and Jacobsen (2008) focuses on the way of incorporating a priori knowledge into a grey-box model and lists four major methodologies of grey-box modeling.

The first methodology, constrained black-box identification, originates from the black-box identification framework, where *a priori* knowledge is incorporated by imposing constraints on the model parameters. The following is the justification of this approach: a simple continuous model can be transformed into a corresponding discrete time model and known restrictions of the continuous model, such as process stability and the step response, can be used to define limits placed on the static gain and the time constants, which are imposed on the parameters of the discrete model.

The second methodology, semi-physical modeling, makes use of case specific nonlinear transformations of measured input/output process signals (Sohlberg and Jacobsen, 2008), e.g., a nonlinear sensor characteristic. A Wiener–Hammerstein model is representative of this class of models (Ljung, 1999). Transformed signals are then used to estimate unknown parameters of a linear black-box model, for instance an ARMAX-type model.

The third methodology, namely, analytical modeling, is based on a basic model originating from mathematical relations derived from the first-principle equations. Analytical modeling deals with lumped and distributed parameter systems. Lumped-parameter models are most commonly considered in this approach. Nonetheless, spatially distributed phenomena have a significant influence on many chemical and thermodynamic processes, for instance, on those involving mass or energy transport by convection or diffusion.

Mathematical representation of a distributed-parameter system involves Partial Differential Equations (PDEs) (Sohlberg and Jacobsen, 2008). A specific challenge in calibrating and validating PDEs is that of distinguishing between model reduction errors and model–data discrepancies (Sohlberg and Jacobsen, 2008; Ljung, 1999). Calibration and validation of PDE models commonly involves discretization of spatial variables

leading to a model represented as a system of Ordinary Differential Equations (ODEs) (Funkquist, 19997; Liu, 2005; Liu and Jacobsen, 2004). The approach was used experimentally by Gewitz (2005) and Weyer *et al.* (2000) in application to modeling a heat exchanger.

In this work, a heat exchanger was divided into two sections, high and low temperature. The temperature in each section was taken as a state variable along with the following physical assumptions: (i) the amount of heat transferred to the surrounding environment is negligible, (ii) heat conduction in the flow direction in both plates and fluids is absent, (iii) each section is characterized by a uniform temperature distribution and constant specific heat capacity (Gewitz, 2005).

Fluids at different initial temperatures are allowed to pass, as a counter-flow, through parallel chambers containing metal plates. In the process, the heat is conducted between the fluid "sections". A similar approach has been applied to a linearized, distributed model of a heat exchanger and presented by Bonivento *et al.* (2001).

The fourth of the methodologies listed at the beginning of this section, hybrid modeling, separates the model into a white/transparent box part, a first-principle equation model, and a black-box part represented by a data-fitted neuro-fuzzy (or similar) model. Thanks to using a hybrid model, the predictions tend towards results obtainable from the first-principle model when new operating conditions are encountered and, additionally, the data-based models are used in already encountered and known operating conditions (Penha and Hines, 2002).

There are two major methodologies: the "serial approach" and the "parallel approach" (Penha and Hines, 2002). The former uses a data-based model to construct missing inputs or parameter estimates of the first-principle model, while the latter uses a nonlinear data-driven dynamical structure (e.g., neural nets, fuzzy sets, evolutionary computing) to model nonlinearities, disturbances or other processes not accounted for in the first-principle model. In the serial hybrid modeling approach, nonlinear system identification methods are used to estimate parameters of first-principle models, which are then used to model the system. Estimated parameters may be unknown, unmeasurable, changing with time or otherwise uncertain.

In the parallel hybrid modeling approach, a nonlinear system identification method is used to predict the residuals not explained by the first-principle model (Penha and Hines, 2002). Predicted residuals are added to the output of the first-principle model during its operation, resulting in a total prediction much closer to the response of the actual system. As shown by Penha and Hines (2002), both the physical model and the parallel hybrid modeling architecture are capable of modeling a heat exchanger. The physical model did not perform well at all in the steady state conditions, therefore standard neural network architectures (multi-layer perceptrons) were used to improve its performance. For comparison purposes, the authors developed a hybrid series model and compared its performance with the parallel hybrid model described by Penha and Hines (2002). An overview of the grey-box model categories discussed herein is presented (Bohlin, 2006; Korbicz *et al.*, 1993; Pearson and Pottmann, 2000; Sohlberg and Jacobsen, 2008).

3. First-principle model of a feedwater heater

Investigation of the dynamics of a power plant requires detailed models comprising sub-models representing particular components of a plant. These models are based on first-principle equations (e.g., mass, momentum, and energy balance) that involve phenomenological correlations, like heat transfer coefficients. Such models are commonly utilized to gain an understanding of physical processes, in process efficiency optimization and in diagnostics aimed at detection of abnormalities, like gradual or abrupt changes in a process. These models are knowledge models, whereby process dynamics can be understood.

The complexity of these models may be different depending on the modeling purpose, starting from compact, lumped-parameter models capturing only the first-cut dynamics, through moderately complex ones, up to complex, large-scale, distributed-parameter models (Hangos and Cameron, 2001). In this context, a feedwater heater, as one of the components of a power plant, requires at least a moderately complex model to capture its fundamental thermodynamic processes.

The model applies three categories of parameters: geometrical, physical and phenomenological. Geometrical parameters are deduced from the construction or operational documentation. Nevertheless, models with deduced parameters are always biased, to some extent, by imprecision caused by the fact that a lumped-geometry model is used instead of a distributed-geometry one. The level of inaccuracy that is acceptable depends on the modeling purpose, available geometrical data and user preferences.

Physical parameters can also be defined based on available documentation and, similarly to geometrical parameters, are also prone to the same error type during aggregation of a distributed-parameter representation into a lumped-parameter representation, e.g., a spatially distributed mass of a heater construction.

The third category, phenomenological parameters, describe physical processes, such as transfer or loss of energy, and are typically functions of other sub-parameters, such as the type of heat conduction surface, type of fluid, its density and velocity of the fluid flow. Under the assumption that all the other model parameters, i.e., geometrical and physical, are known, the system identification

methodology, allows phenomenological parameters to be adjusted based on operational data.

This section describes a moderately complex model of a feedwater heater, in which four phenomenological parameters, i.e., steam-feedwater, steam-metal, condensate-feedwater, and condensate-metal heat transfer coefficients, are tunable. The model of a feedwater heater proposed herein provides a satisfactory compromise between the numerical performance and modeling accuracy. The model involves a simplified model of a steam path, in which the desuperheating zone is neglected, based on the assumption that the steam turns into the condensing phase immediately after coming into the heater cavity. Therefore, the model consists of two control volumes, i.e., a combined desuperheating and condensing volume, and a subcooling volume (Fig. 1).

The following are the assumptions underlying the steam flow path model (Flynn, 2000). Negligible are: (i) the exchange of the heat between the cavity and the external environment, (ii) the accumulation of the heat in the water and (iii) the exchanges of the energy and the mass, caused by the surface phenomena at the interface between the condensing and the subcooling areas. Additionally, it is assumed that all the areas where the exchange of the heat takes place are variable and depend on the desuperheating-condensing and subcooling volumes, and (iv) the pressure in the cavity is constant and uniformly distributed and equal to the steam pressure at the inlet. Moreover, the enthalpy is averaged over each of the areas based on the boundary conditions of each heater chamber.

The following are the assumptions underlying the model of the feedwater flow path (Flynn, 2000). The feedwater is in a liquid state and in a subcooling condition. The pressure of the fluid in the tube-bundle equals the pressure of the feedwater at the inlet. The physical properties of the tube-bundle metal are uniform, and the longitudinal heat conduction in both the pipe metal and the fluid is negligible.

The model of the heater uses equations of conservation of the mass of the drain water, conservation of the mass of the water and the steam, as well as conservation of the energy of the subcooled water, in order to describe the behavior of the fluid inside the cavity of the heater. Particular control volumes are defined by the i-th input and i-th output parameters at the boundaries n and $n+1$, respectively. For instance, the control volume V_{12} is characterized by the input temperature T_1 and the output temperature T_2. The heat energy flow through the n-th boundary of the j-th control volume is given as the product of the fluid enthalpy and the mass flux,

$$\dot{Q}_n = h_n \cdot \dot{m}_n. \tag{1}$$

The transfer of heat energy from the i-th to the i-th control volume of the steam flow path and the j-th to the j-th control volume of the feedwater flow path is given using logarithmic means of the temperature difference for counterflow conditions,

$$\dot{Q}_{ii-jj} = k_{ii-jj} \cdot A_{ii-jj} \cdot \frac{(T_i - T_j)_n - (T_i - T_j)_{n+1}}{\ln(\frac{(T_i - T_j)_n}{(T_i - T_j)_{n+1}})}, \tag{2}$$

where the heat exchange area is a nonlinear function of the heater height (volume of the heater cavity). The transfer of the heat energy from the i-th to the i-th control volume of the steam flow path and the mass of the metal of the heater shell is given by the following expression:

$$\dot{Q}_{ii-m} = k_{ii-m} \cdot A_{ii-m} \cdot \frac{(T_i - T_m)_n - (T_i - T_m)_{n+1}}{\ln(\frac{(T_i - T_m)_n}{(T_i - T_m)_{n+1}})}. \tag{3}$$

The assumption of the uniformity of the enthalpy distribution in each control volume of the heater is expressed by the equation of internal energy in a particular control volume

$$H_{jj} = m_{jj} \cdot (h_n - h_{n+1}). \tag{4}$$

Particular heat exchange areas of the combined desuperheating-condensing and draining volumes are obtained from the following formulas:

$$\begin{cases} A_{12} = f_A(V_{12}), \\ A_{23} = A_{\text{tot}} - f_A(V_{12}). \end{cases} \tag{5}$$

The level of the condensate inside the heater is calculated from

$$x = \frac{V_{23} - V_{230}}{A_{\text{con}}}, \tag{6}$$

where A_{con} is the area of a condensate surface in a heater cavity and V_{230} is the nominal (reference) height of the condensate volume.

3.1. Steam flow path. Equations (8) and (10), describing conservation of the energy in the desuperheating-condensing and draining volumes, are formulated separately for the volumes V_{12} and V_{23}, respectively. Equations (7) and (9), describing conservation of the mass in the desuperheating-condensing and draining volumes, are formulated separately for the mass of steam m_{12} and mass of water (condensate) m_{23}, respectively. The system of equations of the steam flow path is as follows:

$$\frac{\mathrm{d}m_{12}}{\mathrm{d}t} = \dot{m}_1 - \dot{m}_2, \tag{7}$$

$$\frac{\mathrm{d}H_{12}}{\mathrm{d}t} = \dot{Q}_1 - \dot{Q}_2 - \dot{Q}_{12-56} - \dot{Q}_{12-m}, \tag{8}$$

$$\frac{\mathrm{d}m_{23}}{\mathrm{d}t} = \dot{m}_2 - \dot{m}_3, \tag{9}$$

$$\frac{\mathrm{d}m_{23}}{\mathrm{d}t} = \dot{Q}_2 - \dot{Q}_3 - \dot{Q}_{23-45} - \dot{Q}_{23-m}. \tag{10}$$

The term $\dot{Q}_3$ represents the outgoing energy rate of the condensate from the actual heater to the upstream

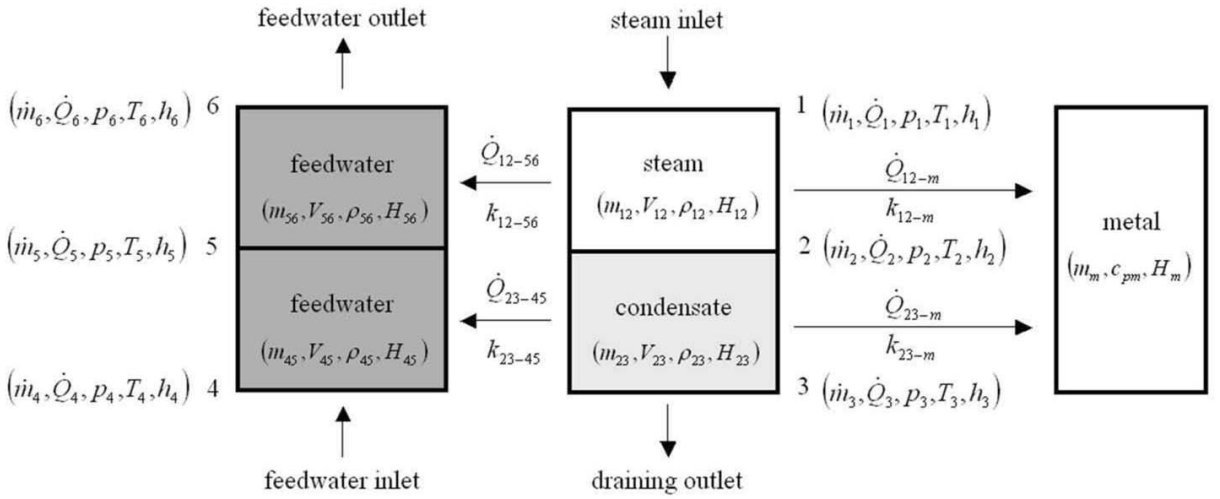

Fig. 1. Schematic representation of the model of a four-volume heater.

heater corrected by the term of the incoming energy rate of the condensate from the downstream heater,

$$\begin{aligned}\dot{Q}_3 &= \dot{Q}_3 - \dot{Q}_{\text{downstream}} \\ &= \dot{Q}_3 - h_{\text{downstream}} \cdot \dot{m}_{\text{downstream}},\end{aligned} \tag{11}$$

where $\dot{m}_3$ is the outgoing mass rate of the condensate from the actual heater to the upstream heater corrected by the term of the ingoing mass rate of the condensate from the downstream heater,

$$\dot{m}_3 = \dot{m}_3 - \dot{m}_{\text{downstream}}. \tag{12}$$

The volume V_{12} and the pressure p_{12} of the condensate inside the steam cavity were selected as the state variables and are related to the mass and the internal energy via the following matrix of partial derivatives:

$$\begin{aligned}\begin{bmatrix}\dfrac{\mathrm{d}m_{12}}{\mathrm{d}t}\\[2mm] \dfrac{\mathrm{d}H_{12}}{\mathrm{d}t}\end{bmatrix} &= \begin{bmatrix}\dfrac{\partial m_{12}}{\partial V_{12}} & \dfrac{\partial m_{12}}{\partial p_{12}}\\[2mm] \dfrac{\partial H_{12}}{\partial V_{12}} & \dfrac{\partial H_{12}}{\partial p_{12}}\end{bmatrix} \cdot \begin{bmatrix}\dfrac{\mathrm{d}V_{12}}{\mathrm{d}t}\\[2mm] \dfrac{\mathrm{d}p_{12}}{\mathrm{d}t}\end{bmatrix} \\ &= \begin{bmatrix}e_{11} & e_{12}\\ e_{21} & e_{22}\end{bmatrix} \cdot \begin{bmatrix}\dfrac{\mathrm{d}V_{12}}{\mathrm{d}t}\\[2mm] \dfrac{\mathrm{d}p_{12}}{\mathrm{d}t}\end{bmatrix}\end{aligned} \tag{13}$$

Equations (7) and (8) take, upon substitution, the following form:

$$\begin{aligned} e_{11} \cdot \frac{\mathrm{d}V_{12}}{\mathrm{d}t} + e_{12} \cdot \frac{\mathrm{d}p_{12}}{\mathrm{d}t} &= \dot{m}_1 - \dot{m}_2, \\ e_{21} \cdot \frac{\mathrm{d}V_{12}}{\mathrm{d}t} + e_{22} \cdot \frac{\mathrm{d}p_{12}}{\mathrm{d}t} &= \dot{Q}_1 - \dot{Q}_2 - \dot{Q}_{12-56} \\ &\quad - \dot{Q}_{23-45}, \end{aligned} \tag{14}$$

where the individual elements of the partial derivative matrix are given by the following expressions:

$$\begin{aligned} e_{11} &= \frac{\partial m_{12}}{\partial V_{12}} = \frac{\partial (m_{12} \cdot V_{12})}{\partial V_{12}} = \rho_{12} + \frac{\partial \rho_{12}}{\partial V_{12}} \cdot V_{12}, \\ e_{12} &= \frac{\partial m_{12}}{\partial p_{12}} = \frac{\partial \rho_{12}}{\partial p_{12}} \cdot V_{12} + \frac{\partial V_{12}}{\partial p_{12}} \cdot \rho_{12}, \\ e_{21} &= \frac{\partial H_{12}}{\partial V_{12}} = \frac{\partial (\rho_{12} V_{12} h_{12})}{\partial V_{12}} \\ &= \rho_{12} h_{12} + \frac{\partial \rho_{12}}{\partial V_{12}} \cdot h_{12} V_{12} + \frac{\partial h_{12}}{\partial V_{12}} \cdot \rho_{12} V_{12}, \end{aligned}$$

$$\begin{aligned} e_{22} &= \frac{\partial H_{12}}{\partial p_{12}} = \frac{\partial (\rho_{12} V_{12} h_{12})}{\partial p_{12}} \\ &= \frac{\partial \rho_{12}}{\partial p_{12}} \cdot V_{12} h_{12} + \frac{\partial V_{12}}{\partial p_{12}} \cdot \rho_{12} h_{12} \\ &\quad + \frac{\partial h_{12}}{\partial p_{12}} \cdot \rho_{12} V_{12} - V_{12}. \end{aligned} \tag{15}$$

The assumption that

$$\frac{\partial \rho_{12}}{\partial V_{12}} \equiv 0, \quad \frac{\partial V_{12}}{\partial p_{12}} \equiv 0$$

yields

$$\begin{aligned} e_{11} &= \frac{\partial m_{12}}{\partial V_{12}} = \rho_{12}, \\ e_{12} &= \frac{\partial m_{12}}{\partial p_{12}} = \frac{\partial \rho_{12}}{\partial p_{12}} = V_{12}, \\ e_{21} &= \frac{\partial H_{12}}{\partial V_{12}} = \rho_{12} h_{12} - p_{12}, \\ e_{22} &= \frac{\partial H_{12}}{\partial p_{12}} = V_{12}\Big(h_{12} \frac{\partial \rho_{12}}{\partial p_{12}} + \rho_{12} \frac{\partial h_{12}}{\partial p_{12}}\Big) - V_{12} \end{aligned} \tag{16}$$

and, additionally,

$$V_{12} = V_{\text{total}} - V_{23}, \quad \mathrm{d}V_{12} = -\mathrm{d}V_{23}. \tag{17}$$

The mass of the water in the condensate cavity is determined from the assumption written as follows:

$$\begin{aligned} &\text{If} \quad \frac{\mathrm{d}m_{12}}{\mathrm{d}t} = \dot{m}_1 - \dot{m}_2 \text{ and } \frac{\mathrm{d}m_{23}}{\mathrm{d}t} = \dot{m}_2 - \dot{m}_3, \\ &\text{then} \quad \frac{\mathrm{d}m_{23}}{\mathrm{d}t} = \dot{m}_1 - \dot{m}_3 - \frac{\mathrm{d}m_{12}}{\mathrm{d}t}. \end{aligned} \tag{18}$$

Variables obtained from (18) are substituted to (14),

$$\begin{aligned} \dot{m}_3 - \dot{m}_2 &= e_{11}\frac{\mathrm{d}V_{12}}{\mathrm{d}t} + e_{12}\frac{\mathrm{d}p_{12}}{\mathrm{d}t}, \\ \dot{m}_3 h_3 - \dot{m}_2 h_2 - \dot{Q}_{12-m} - \dot{Q}_{23-m} &= e_{21}\frac{\mathrm{d}V_{12}}{\mathrm{d}t} + e_{22}\frac{\mathrm{d}p_{12}}{\mathrm{d}t}. \end{aligned} \tag{19}$$

The unknowns are determined as follows:

$$\begin{aligned} \mathrm{d}p_{12} = {} & \frac{1}{e_{22} - e_{12}h_2}\Big[m_3(h_3 - h_2) - (e_{21} \\ & - e_{11}h_2)\frac{\mathrm{d}V_{12}}{\mathrm{d}t} - \dot{Q}_{12-m} - \dot{Q}_{23-m}\Big] \\ \dot{m}_2 = {} & \frac{1}{e_{22} - e_{12}h_2}(e_{12}e_{21} - e_{11}e_{22})\frac{\mathrm{d}V_{12}}{\mathrm{d}t} \\ & + \Big[e_{12}(\dot{Q}_{12-m} - \dot{Q}_{23-m}) - (e_{12}h_3 - e_{22})\dot{m}_3\Big]. \end{aligned} \tag{20}$$

A heat transfer from the heater cavity to the metal of the heater shell is formulated with the use of the energy conservation law,

$$\frac{\mathrm{d}H_m}{\mathrm{d}t} = \dot{Q}_{12-m} + \dot{Q}_{23-m}, \tag{21}$$

where

$$H_m = m_m \cdot c_{pm} \cdot T_m. \tag{22}$$

3.2. Feedwater flow path. Equations

$$\frac{\mathrm{d}H_{45}}{\mathrm{d}t} = \dot{Q}_4 - \dot{Q}_5 + \dot{Q}_{23-45}, \tag{23}$$

$$\frac{\mathrm{d}H_{56}}{\mathrm{d}t} = \dot{Q}_5 - \dot{Q}_6 + \dot{Q}_{12-56}, \tag{24}$$

are formulated based on the conservation of the energy in the feedwater volumes corresponding to the desuperheating-condensing and draining with the assumption of uniformity of the feedwater density distribution.

3.3. Modeling object. A high-pressure heater, denoted by XW1 in Fig. 2, was used as a reference system, characterized by the operational and constructional data presented in Table 1. The values of the phenomenological model parameters, depending on the estimation case, are given in Sections 5.3–5.4 in Tables 5–6. The remaining values were taken from the operational documentation. The list of input-output variables and calculated variables is presented in Tables 2 and 3, respectively.

4. Method for adjusting parameters of the first-principle model

The heater model is represented as a set of non-linear state-space equations formulated in the continuous-time domain. The objective of the estimation is to minimize the error function between the measured signals and model responses by means of an iterative numerical technique (Ljung, 1999). The function describing the error has to be positive and decreasing. The procedure of model tuning consists of two in-a-loop phases: (i) simulation of a model by solving differential equations numerically in Simulink (Mathworks, 2007), and (ii) numerical minimization in the parameter space with respect to an error-related criterion function using the Matlab Optimization Toolbox (Mathworks, 2007). After each simulation of the model for fixed-length input signals, the simulated output data are sampled and the criterion is re-evaluated to calculate a new set of model parameters. Interested readers may find more information concerning available toolboxes that support identification of first-principle models in the works of Ljung (1999) and Bohlin (2006).

The following structure of nonlinear state-space equations provides a general representation of the heater model:

$$\begin{aligned} \frac{\mathrm{d}}{\mathrm{d}t}x(t) &= f(t, x(t), u(t), w(t); \theta), \\ y(t) &= h(t, x(t), u(t), v(t); \theta), \\ x(0) &= x_0, \end{aligned} \tag{25}$$

where the vector $f(\cdot)$ is a nonlinear, time-varying function of the state vector $x(t)$ and the control vector $u(t)$, while vector $h(\cdot)$ is a nonlinear measurement function, $w(t)$ and $v(t)$ are sequences of independent random variables and θ denotes a vector of unknown parameters. The predictor resulting from the model (25) takes the form

$$\hat{y}(t|\theta) = g(t, Z^{t-1}; \theta), \tag{26}$$

while the prediction error equation has the form

$$\varepsilon(t, \theta) = y(t) - g(t, Z^{t-1}; \theta). \tag{27}$$

The sum of squared errors is used as an error criterion. This problem is known in numerical analysis as the "nonlinear least-squares problem" (Ljung, 1999). The objective of the estimation is to minimize the error function $V_N(\theta)$ by means of an iterative numerical technique. The error function $V_N(\theta)$ has the form

$$V_N(\theta, Z^N) = \frac{1}{N}\sum_{t=1}^{N}\frac{1}{2}\varepsilon^2(t, \theta). \tag{28}$$

Three methods of minimizing the error function (28) are available for nonlinear grey-box modeling. These

Table 1. Parameters of the high-pressure heater XW1 used in simulation.

Type of parameter	Parameter	Symbol	Unit	Value
Geometrical	Heat exchange area—steam	A_{12}	$[\mathrm{m}^2]$	$f_A(V_{12})$
	Heat exchange area—condensate	A_{23}	$[\mathrm{m}^2]$	$A_{\mathrm{tot}} - f_A(V_{12})$
	Overall heat exchange area	A_{tot}	$[\mathrm{m}^2]$	600
	Steam and condensate volume	$V_{12} + V_{23}$	$[\mathrm{m}^3]$	2.9
	Feedwater volume	$V_{45} + V_{56}$	$[\mathrm{m}^3]$	4
	Heater height	x	[m]	10
Physical	Mass of the metal of a heater	m_m	[kg]	35500
	Specific heat of a metal	c_{pm}	$[\mathrm{J/kg \cdot K}]$	$500 \cdot 10^{-3}$
Phenomenological parameters	Heat transfer coefficient steam to feedwater	k_{12-56}	$[\mathrm{kW \cdot m^{-2} \cdot K^{-1}}]$	Table 5+6
	Heat transfer coefficient condensate to feedwater	k_{23-45}	$[\mathrm{kW \cdot m^{-2} \cdot K^{-1}}]$	Table 5+6
	Heat transfer coefficient steam to metal	k_{12-m}	$[\mathrm{kW \cdot m^{-2} \cdot K^{-1}}]$	Table 5
	Heat transfer coefficient condensate to metal	k_{23-m}	$[\mathrm{kW \cdot m^{-2} \cdot K^{-1}}]$	Table 5
PID settings	Proportional	P	$[-]$	0.8
	Integration	I	[s]	53
	Derivative	D	$[\mathrm{s}^{-1}]$	0

Table 2. List of input and output variables of the two-volume heater model.

Input signals		Output signals	
Signal name	Unit	Signal name	Unit
Steam flow rate $\dot{m}_1$	[kg/s]	Condensate flow rate $\dot{m}_3$	[kg/s]
Steam temperature T_1	[C°]	Condensate temperature T_3	[C°]
Steam pressure p_1	[MPa]	Condensate pressure p_3	[MPa]
Feedwater flow rate $\dot{m}_3$	[kg/s]	Feedwater flow rate $\dot{m}_6 = \dot{m}_3$	[kg/s]
Feedwater temperature T_3	[C°]	Feedwater temperature T_6	[C°]
Feedwater pressure p_3	[MPa]	Feedwater pressure $p_6 = p_3$	[MPa]
Reference (set-point) condensate level x_{conref}	[m]	Condensate level x_{con}	[m]
Downstream condensate flow rate $\dot{m}_{\mathrm{downstream}}$	[kg/s]		
Downstream condensate temperature $T_{\mathrm{downstream}}$	[C°]		
Downstream condensate pressure $p_{\mathrm{downstream}}$	[MPa]		

Table 3. List of calculated (auxiliary) variables of the four-volume heater model.

Variable	Symbol	Unit
Steam volume	V_{12}	$[\mathrm{m}^3]$
Condensate volume	V_{23}	$[\mathrm{m}^3]$
Feedwater volume corresponding to steam volume	V_{56}	$[\mathrm{m}^3]$
Feedwater volume corresponding to condensate volume	V_{45}	$[m^3]$
Condensate level	x_0	[m]

are (i) direct search, (ii) first-order, and (iii) second-order methods. Direct search methods use only the value of the function to find the minimum. The first-order method uses the information provided by the first derivatives (gradient) of the error function, while the second-order method uses both information regarding the first and the second order derivatives (gradient and Hessian form) of the error function.

5. Model validation and discussion of results

This section presents the tuning process of the continuous-time heater model formulated in Section 3 in Simulink, along with the use of the Simulink Parameter Estimation toolbox to adjust its phenomenological parameters.

The final application goal of the developed identification methodology is the virtual power plant model, including all the necessary flow paths required to simulate the basic functionality of a power unit, i.e., a boiler, a turbine, a net load, and a feedwater regeneration system. For the purpose of generic investigations, a model isolated from the system is required. However, flow measurements are only available for larger parts of the system. For example, the feedwater flow rate is captured only after the turbine and before the boiler. This implies a need for reconstructing missing signals from others with the use of a static flow coefficient.

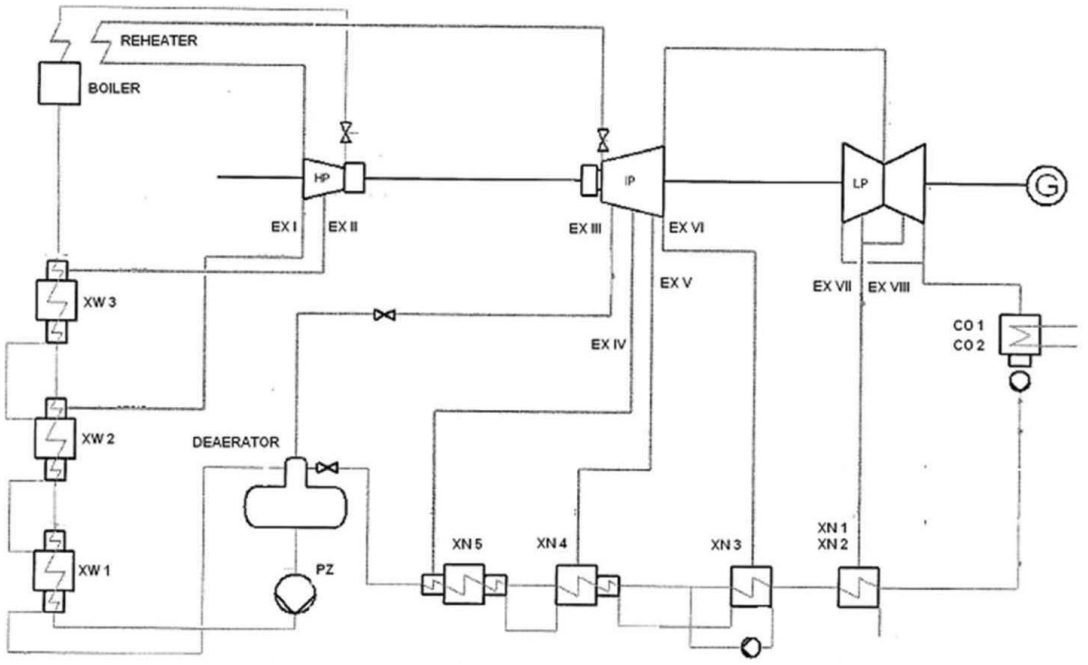

Fig. 2. Functional scheme of a power block (EX: steam extraction port, XW: high pressure heater, XN: low pressure heater, CO: condenser, PZ: main pump).

5.1. Description of a feedwater installation. The heater, denoted by XW1 in Fig. 2, is a part of a feedwater regeneration system in which feed pumps pass the condensed steam (feedwater) from a condenser through heater banks, supplied by the steam extracted from the high, intermediate and low-pressure sections of a steam turbine. The condensate is pumped to the deaerator, through the bank of low-pressure heaters XN1, XN2, XN3, XN4 and XN5, and further from the deaerator to the steam generator (boiler) through the bank of high-pressure heaters XW1, XW2 and XW3.

The drainage system of the feedwater heater consists of a drain removal path from each heater. The normal drain flow path is cascaded to the next lower stage heater, and the alternate path is diverted to the condenser. The heaters XN1 and XN2 assembled in the condensers are in continuous operation with the condensers CO1 and CO2. When the turbine is loaded at a given rate, steam is allowed to enter the bank of high-pressure heaters through extraction outlets and pipelines denoted by III, II and I to the heaters XW3, XW2 and XW1, respectively. Regulatory control loops of the condensate level control are coupled to the power unit controller. The control system consists of the PID controller, which enables the condensate level variation to be compensated and maintains its constant level in the subcooling zone. In order to increase the maximum power of the turbine and to maintain the required margin of controllable power of the turbine under high load conditions, the steam pressure control valves were installed in the steam pipeline between the extraction ports EX I and EX II to the heaters XW 2 and XW3 (Fig. 2). The valves enable the temperature of the feedwater to be controlled by regulating the pressure of the steam entering the heater.

The following signals are available: the condensate level, steam pressure inside the heater cavity, feedwater flow rate, the temperature of the feedwater and condensate. The condensate level signal was not used in adjusting heater parameters since its value is almost constant and dynamics are much faster than the thermal process. The steam pressure signal was used in order to reconstruct the dynamics of the steam flow rate into the heater cavity from the turbine extraction port. If the internal pressure inside the four-volume heater model, $p_{12} = p_{23}$, is greater than or equal to or the inlet pressure p_1, then the inlet steam flow rate approaches zero, complying with the formula

$$\dot{m}_1 = \begin{cases} \alpha \cdot (p_{12} - p_1)^{\gamma} & \text{if} \quad p_{12} < p_1, \\ 0 & \text{if} \quad p_{12} \geq p_1, \end{cases} \tag{29}$$

where α is the discharge coefficient and γ is a coefficient dependent on the character of the flow. The inlet and outlet flows of the feedwater are equal due to the assumption of constant density. Finally, the signals of the temperature of feedwater and condensate were used as reference data for optimization algorithms.

The performance of the parameter adjustment procedure is evaluated by visual inspection of a plot (Figs. 5, 7 and 9, bottom panels) or by analyzing the value of the Pearson correlation coefficient.

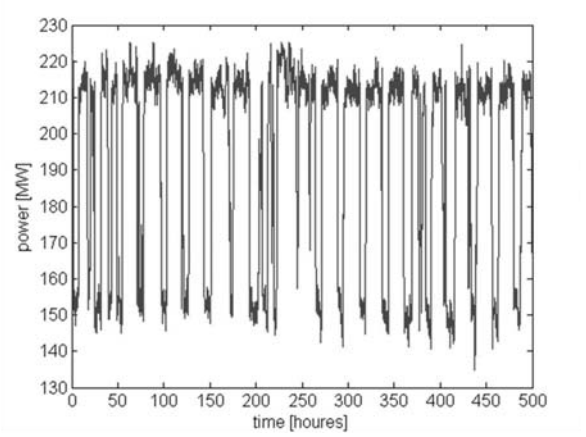

Fig. 3. Power rate variability over operating time of a power unit.

5.2. Input-output signals. The load of a power unit is subjected to daily/weekly fluctuations from low to high (Fig. 3). As a consequence, the data are concentrated around two operating points, namely 155 MW and 215 MW, while the full operating range is not sufficiently covered. The data have a multi-modal distribution as a mixture of Gaussian distributions corresponding to those operating points (Fig. 4).

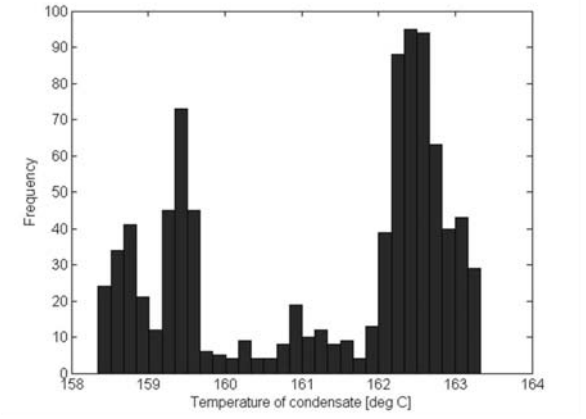

Fig. 4. Multi-modal distribution of an output signal of a heater model (temperature of the condensate).

5.3. Settings of the optimization and simulation algorithms. The simulation and optimization settings used in the parameter adjustment process are presented in Table 4. The Newton–Gauss method implemented as the `lsqnonlin`$(\cdot)$ routine in the Optimization Toolbox (Mathworks, 2007) was used to minimize the function describing the error in the measurement signals and model responses.

The simulation model is run in continuous time. After each run of the model for fixed-length input signals (901 samples), the simulated output data are sampled ($T_s = 60$ s) and the criterion function is evaluated to determine a new set of model parameters. The number of runs is limited by the parameter `MaxIter`, see Table 4.

5.4. Adjustment of model parameters based on operational data. The simulation model considered in this section consists of a heater model including an equivalent model of a PID controller opening the drainage valve. The settings of the controller were read directly from the operational documentation. Geometrical and physical parameters of the heater model (Table 1) were also extracted from the operational documentation and are assumed to be known. The four phenomenological parameters, namely, k_{12-m}, k_{23-m}, k_{12-56} and k_{23-45} (Fig. 5), which, by definition, remain constant over a wider range of operating conditions, are identified. The range of operating conditions corresponds to that of the power ratio of the turboset, i.e., between 140 and 225 MW. The procedure of numerically adjusting these parameters was executed to find the values that ensured the best fit of the heater model to the data. The model was run and tested on a PC with an Intel Core i7 CPU 3 GHz and 6 GB RAM under Microsoft Windows 7 Edition. Matlab v. 7.8 (R2009a) was used. Results are presented in Table 5 and, additionally, the fit of the model to data is presented graphically in Fig. 5, the bottom panel). The model reproduces the trend in the condensate and the feedwater temperatures with good accuracy.

The quality of the fit of the model is assessed by a measure based on the Pearson correlation coefficient. Convergence trajectory plots show a stable trend towards constant values of the parameters, which correspond to convergence towards the minimum of the criterion function, within less than 6 iterations (Fig. 5, top panel, and Fig. 6).

The convergence is further confirmed by clear trends in sequences of the first-order difference of parameter values, additionally illustrating the speed in which the algorithm converges to the solution. First-order difference sequences approach zero, indicating convergence in a few iterations (Fig. 5, middle panel). The final values of heat exchange coefficients are not affected by the initial conditions (Table 5).

5.5. Adjustment of reduced model parameters based on operational data. The application goal is to use the feedwater model as a part of the on-line monitoring system of a power unit. In this application, the model traces operational data and adjusts the model parameters assuming quasi steady-state operation of the units. This assumption allows the process of accumulation of thermal energy in the housing metal to be neglected. The thermal inertia of the heat transfer between the steam in the heater cav-

Table 4. Simulation and optimization settings.

Simulation		Optimization (minimization)	
Option	Value	Option	Value
Solver	`ode23tb` (stiff/TR-BDF2)	Gradient type	basic
Max step size	Auto	Algorithm	`lsqnonlin`
Min step size	Auto	Cost type	SSE
Zero crossing control	Disable all	DiffMaxChange	0.1
Relative tolerance	Auto	DiffMinChange	1E-08
Absolute tolerance	Auto	Large scale	true
		MaxIter	28
		RobustCost	False
		TolCon	1E-6
		TolFun	1E-6

Table 5. List of calculated (auxiliary) variables of the four-volume heater model.

	Case A	Case B	Case C	Case D
Initial value k_{23-45}	3	1	4	5
Initial value k_{12-56}	3	1	4	0.2
Initial value k_{23-m}	3	1	0.3	5
Initial value k_{12-m}	3	1	0.3	2
Estimated value k_{23-45}	3.488	3.457	3.456	3.455
Estimated value k_{12-56}	1.658	1.658	1.656	1.657
Estimated value k_{23-m}	0.2345	0.2456	0.2719	0.2731
Estimated value k_{12-m}	0.6347	0.6227	0.2228	0.7495
Model fit (feedwater)	0.84	0.83	0.82	0.82
Model fit (condensate)	0.85	0.85	0.86	0.87
Computation time [min]	120	128	108	125

ity and the metal of the housing is of the order of several minutes and is negligible when compared with the thermal inertia of the heat transfer between the steam and the feedwater, being of the order of the simulation time. Following this assumption, the model can be reduced, neglecting heat accumulation in the housing metal of the feedwater heater. The number of adjustable parameters is two instead of four, i.e., k_{23-56} and k_{23-45}. On the other hand, the measurements of the temperature of the housing metal are difficult to obtain in power plants. They are not captured by data acquisition systems as they are not critical for safety or control process purposes. The results k_{23-56} and k_{23-45} are presented in Table 6 and, additionally, the fit of the model to data is presented graphically in Fig. 7 (bottom panel). The model reproduces the trend in the condensate and the feedwater temperatures with acceptable accuracy.

Convergence trajectory plots show a stable trend towards constant values of the parameters, which correspond to convergence towards the minimum of the criterion function, within less than 6 iterations (Fig. 7, top panel and Fig. 8).

5.6. Adjustment of reduced model parameters based on simulation data. The goal of the simulation study described in this section was to reconstruct the values of model parameters and compare them with known true values. The model configuration was the same as that discussed in Section 5.4. Simulations, for which operational data corrupted by measurement noise were the model input, were performed for two heat transfer coefficients, k_{23-56} and k_{23-45}, based on data generated from these simulations. Zero-mean Gaussian noise with unit standard deviation was added to the simulated output signals, namely, to the condensate and the feedwater temperature signals, to emulate measurement disturbances. The initial values and calculated relative errors between known and reconstructed heat exchange coefficients are presented in Table 7 and, additionally, the fit of the model to data is presented graphically in Fig. 9 (bottom panel). The model

Table 6. Results for the heater XW1.

	Case A	Case B	Case C
Initial value k_{23-45}	2	4	0.2
Initial value k_{12-56}	2	0.2	5
Estimated value k_{23-45}	3.4516	3.4509	3.4484
Estimated value k_{12-56}	1.6568	1.6560	1.6568
Model fit (feedwater)	0.83	0.81	0.81
Model fit (condensate)	0.88	0.88	0.88
Computation time [min]	35	48	55

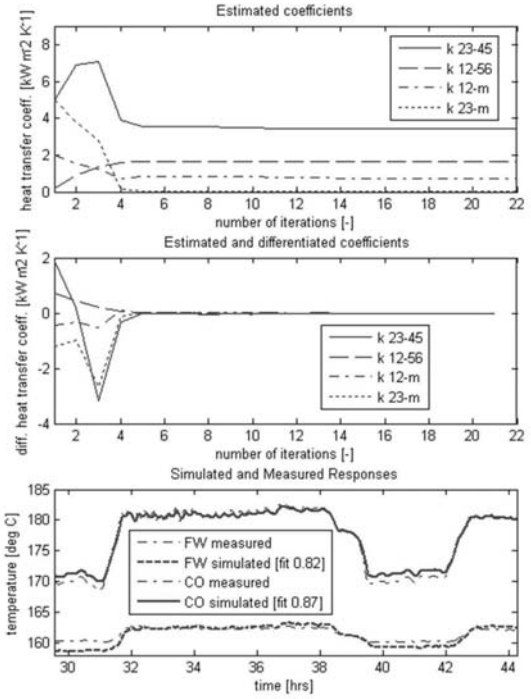

Fig. 5. Graphical representation of the results reported in Table 5 for Case D (FW: feedwater, CO: condensate).

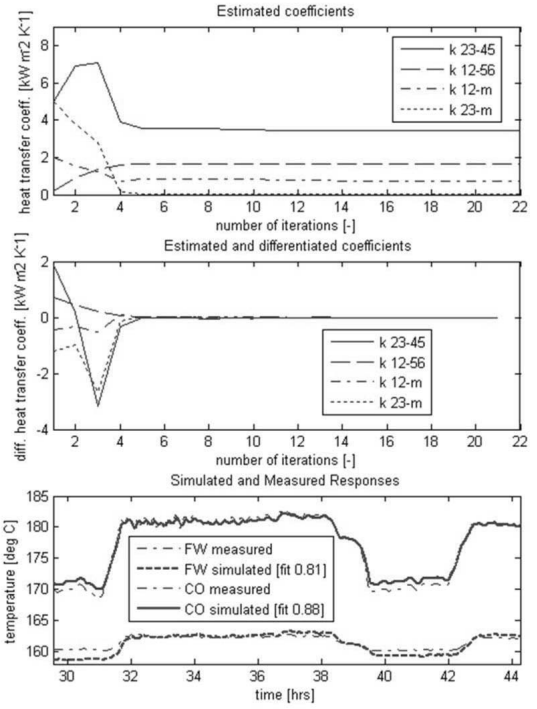

Fig. 7. Graphical representation of the results reported in Table 6 for Case C (FW: feedwater, CO: condensate).

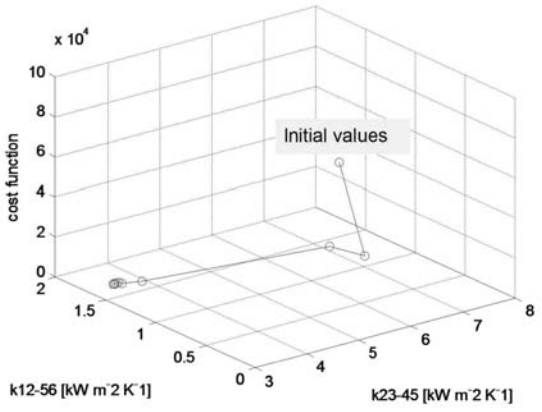

Fig. 6. Trajectory of parameter convergence as a function of the error (Case D, Table 5): points on the line correspond to iterations.

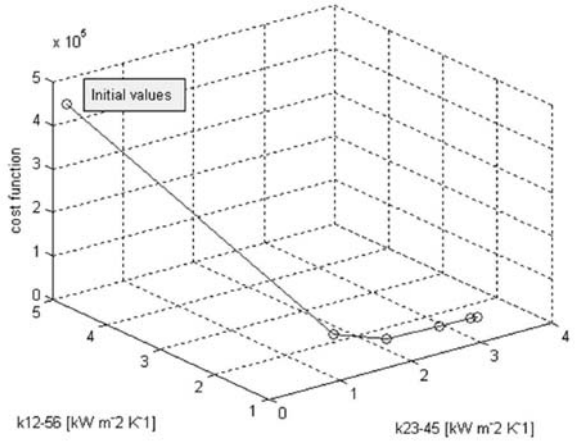

Fig. 8. Trajectory of parameter convergence as a function of the error (Case C, Table 6): points on the line correspond to iterations.

reproduces the trend in the condensate and the feedwater temperatures with excellent accuracy.

This test proved that the proposed system identification procedure was sufficiently robust to estimate model/process parameters even if their values were initially given as far as 100% from the actual (known) values. The fit quality indicator based on the correlation measure is very good, showing that the model achieves an accuracy level of 99%.

6. Conclusions and discussion of the results

6.1. Performance of numerical optimization schemes. Adjusting a model to data is, in most cases, a non-convex optimization problem and the criterion function may have several local minima. It is therefore most natural to use physical insight to provide initial values to ensure robustness and fast convergence of the optimization process, as well as to reduce the dimensionality of the parame-

Table 7. Results for the heater XW1.

	Case A	Case B	Case C
Initial value k_{23-45}	2	4	0.2
Initial value k_{12-56}	2	0.2	5
Estimated value k_{23-45}	3.4516	3.4509	3.4484
Estimated value k_{12-56}	1.6568	1.6560	1.6568
Model fit (feedwater)	0.998	0.997	0.993
Model fit (condensate)	0.999	0.998	0.992
Computation time [min]	30	36	38

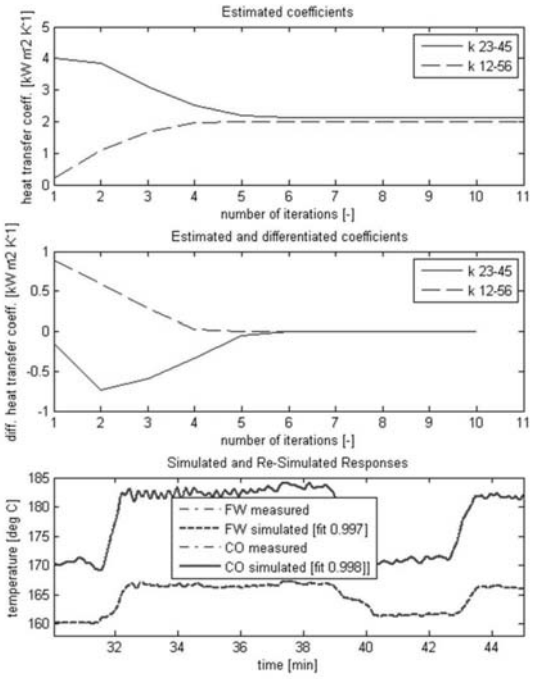

Fig. 9. Graphical representation of the results reported in Table 7 for Case B (FW: feedwater, CO: condensate).

ter space by selecting only those parameter values which are difficult to derive. Using physics-based initial conditions has a significant advantage over blind (random) initialization of the optimization routine and, furthermore, physical meaning of the parameters allows additional constraints to be set on the error function and/or model parameters, narrowing the domain in which the optimum is being searched for. In many cases, it is not possible to obtain initial values of the heat transfer coefficient since the design calculation sheets, typically developed by the manufacturer, are unavailable. Therefore, an inverse algebraic method for solving a linearized version of the equations of the model is used to obtain approximation of the initial conditions. It is also possible to perform rapid and crude calculations based on the static energy balance using an oversimplified model of the heater with only a single heat transfer coefficient and averaged properties of the steam-water mixture inside its cavity.

6.2. Accuracy of the model. The system identification scenario was used to adjust four heat transfer coefficients yielding correlation between the measured and the predicted temperature signals. Moreover, the simplified system identification scenario was used to adjust only the two heat transfer coefficients, while the two remaining ones, responsible for describing the heat transfer between a steam-water mixture and the shell of the heater, were set to zero. The correlation between measured and predicted temperature signals is presented in Tables 5–7. Furthermore, visual inspection of graphs also confirms that the obtained correlations are good.

7. Summary

The paper proposes and defines a first-principle model of a feedwater heater and shows the results of model validation obtained for selected operational and purely numerical datasets. The model offers physical insight and sufficient numerical performance to be applicable in understanding underlying physical phenomena, designing control systems and optimizing processes. The novelty of this work is the method of utilizing operational data to adjust phenomenological parameters of the model of a feedwater heater derived from physical laws. The model, as presented herein, is a natural extension of the static energy balance valid under steady-state operating conditions to a dynamic form valid under transient operating conditions. Thanks to formulating the model as a generalization of a static energy balance, heat transfer coefficients obtained in the static case are adequate as initial values for model adjustment (optimization) algorithms. Moreover, simulation results generated by the model under operating conditions correspond to static prediction performed with the use of an energy balance of the power unit.

References

Barszcz, T. (2007). Virtual power plant in condition monitoring of power generation unit, *Proceedings of the 20th International Congress on Condition Monitoring and Diagnostic Engineering Management, Faro, Portugal*, pp. 1–10.

Barszcz, T. and Czop, P. (2007). *Methodologies and Applications of Virtual Power Plant: New Environment for Power Plant Elements Modeling*, Institute of Sustainable Technologies, Radom.

Bohlin, T. (2006). *Practical Grey-box Process Identification: Theory and Applications (Advances in Industrial Control)*, Springer-Verlag, London.

Bonivento, C., Castaldi, P. and Mirotta, D. (2001). Predictive control vs. pid control of an industrial heat exchanger, *Proceeding of the 9th IEEE Mediterranean Conference on Control and Automation, Dubrovnik, Croatia*, pp. 27–29.

Bradatsch, T., Gühmann, C., Röpke, K., Schneider, C. and Filbert, D. (1993). Analytical redundancy methods for di-

agnosing electric motors, *Applied Mathematics and Computer Science* **3**(3): 461–486.

Flynn, D. (2000). *Thermal Power Plants. Simulation and Control*, Institution of Electrical Engineers, London.

Funkquist, J. (1997). Grey-box identification of a continuous digester a distributed parameter process, *Control Engineering Practice* (5): 919–930.

Gewitz, A. (2005). EKF-based parameter estimation for a lumped, single plate heat exchanger, `www.cespr.fsu.edu/people/myh/reu_ppt05`.

Hangos, K.M. and Cameron, I. (2001). *Process Modeling and Model Analysis*, Academic Press, London.

Korbicz, J., Kościelny, J., Kowalczuk, Z. and Cholewa, W. (2004). *Fault Diagnosis. Models, Artificial Intelligence, Applications*, Springer-Verlag, Berlin.

Korbicz, J., Uciński, D., Pieczyński, A. and Marczewska, G. (1993). Knowledge-based fault detection and isolation system for power plant simulator, *Applied Mathematics and Computer Science* **3**(3): 613–630.

Li, K. and Thompson, S. (2001). Fundamental grey-box modelling. *Proceedings of the European Control Conference, Oporto, Portugal*, pp. 3648–3653.

Liu, Y. (2005). *Grey-box Identification of Distributed Parameter Systems*, Ph.D. thesis, Signals, Sensors and Systems, KTH, Stockholm.

Liu, Y. and Jacobsen, E. W. (2004). Error detection and control in grey-box modelling of distributed parameter processes, *Proceedings of IFAC DYCOPS7, Boston, MA, USA*, pp. 841–846.

Ljung, L. (1999). *System Identification—Theory for the User*, Prentice Hall, Upper Saddle River NJ.

Mathworks (2007). *Matlab System Identification Toolbox Guide*, The Mathworks Inc., Natick, MA.

Patton, R.J., Frank, P.M. and Clark, R.N. (2000). *Issues of Fault Diagnosis for Dynamic Systems*, Springer-Verlag, London.

Pearson, R.K. and Pottmann, M. (2000). Gray-box identification of block-oriented nonlinear models, *Journal of Process Control* **10**(4): 301–315.

Sierociuk, D. and Dzieliński, A. (2006). Fractional Kalman filter algorithm for the states, parameters and order of fractional system estimation, *International Journal of Applied Mathematics and Computer Science* **16**(1): 129–140.

Sohlberg, B. and Jacobsen, E.W. (2008). Grey box modeling—Branches and experience, *Proceedings of the 17th IFAC World Congress, Seoul, Korea*, pp. 11415–11420.

Upadhyaya, B.R. and Hines, J.W. (2004). On-Line Monitoring and Diagnostics of the Integrity of Nuclear Plant Steam Generators and Heat Exchangers, *Report No. DE-FG07-01ID14114/UTNE-07*, NEER Grant No. DE-FG07-01ID14114, `www.osti.gov/bridge/servlets/purl/832717-6tYnaS/native/`.

Tulleken, H.J. (1993). Grey-box modelling and identification using physical knowledge and Bayesian techniques, *Automatica* **29**(2): 285–308.

Weyer, E., Szederkenyi, G. and Hangos, K.M. (2000). Grey box fault detection of heat exchangers, *Control Engineering Practice* **8**(2): 121–131.

Tomasz Barszcz obtained a Ph.D. degree in 1997 in the field of vibration monitoring systems and a D.Sc. degree in 2009 in control and robotics. Since 2000 he has been employed at the Department of Robotics and Mechatronics of the AGH University of Science and Technology in Cracow, Poland. His main field of research combines the development of monitoring system architectures with the development of advanced fault detection and isolation algorithms. He is the author of four books and over 80 papers in this field. Dr. Tomasz Barszcz has been involved in numerous industrial projects with companies from Poland, Switzerland, Germany, UK, China and France. The advanced monitoring and diagnostic technologies developed by the author have been implemented in various industries including power generation (steam, gas and wind), oil and gas, printing, railway transport and automotive.

Piotr Czop received his M.Sc. in 1998 and Ph.D. in 2001, both from the Silesian University of Technology. He worked on R&D projects at Energocontrol Ltd. and AITECH Ltd. in the years 1998–2004. He joined Tenneco Automotive Eastern Europe Ltd. in 2004, where he is responsible for the Control & Measuring Systems Department. His research interests include modeling and identification of multi-domain systems consisting of hydraulic, electrical and mechanical components.

Received: 30 May 2010
Revised: 18 January 2011